

Finite-temperature time-dependent variation with multiple Davydov states

Wang, Lu; Fujihashi, Yuta; Chen, Lipeng; Zhao, Yang

2017

Wang, L., Fujihashi, Y., Chen, L., & Zhao, Y. (2017). Finite-temperature time-dependent variation with multiple Davydov states. *The Journal of Chemical Physics*, 146(12), 124127-.

<https://hdl.handle.net/10356/83491>

<https://doi.org/10.1063/1.4979017>

© 2017 American Institute of Physics (AIP). This paper was published in *The Journal of Chemical Physics* and is made available as an electronic reprint (preprint) with permission of American Institute of Physics (AIP). The published version is available at: [<http://dx.doi.org/10.1063/1.4979017>]. One print or electronic copy may be made for personal use only. Systematic or multiple reproduction, distribution to multiple locations via electronic or other means, duplication of any material in this paper for a fee or for commercial purposes, or modification of the content of the paper is prohibited and is subject to penalties under law.

Downloaded on 20 Mar 2024 19:18:58 SGT

Finite-temperature time-dependent variation with multiple Davydov states

Lu Wang,^{1,2} Yuta Fujihashi,² Lipeng Chen,² and Yang Zhao^{2,a)}

¹Department of Physics, Zhejiang University, Hangzhou 310027, People's Republic of China

²Division of Materials Science, Nanyang Technological University, Singapore 639798, Singapore

(Received 19 December 2016; accepted 9 March 2017; published online 29 March 2017)

The Dirac-Frenkel time-dependent variational approach with Davydov *Ansätze* is a sophisticated, yet efficient technique to obtain an accurate solution to many-body Schrödinger equations for energy and charge transfer dynamics in molecular aggregates and light-harvesting complexes. We extend this variational approach to finite temperature dynamics of the spin-boson model by adopting a Monte Carlo importance sampling method. In order to demonstrate the applicability of this approach, we compare calculated real-time quantum dynamics of the spin-boson model with that from numerically exact iterative quasiadiabatic propagator path integral (QUAPI) technique. The comparison shows that our variational approach with the single Davydov *Ansätze* is in excellent agreement with the QUAPI method at high temperatures, while the two differ at low temperatures. Accuracy in dynamics calculations employing a multitude of Davydov trial states is found to improve substantially over the single Davydov *Ansatz*, especially at low temperatures. At a moderate computational cost, our variational approach with the multiple Davydov *Ansatz* is shown to provide accurate spin-boson dynamics over a wide range of temperatures and bath spectral densities. *Published by AIP Publishing.* [<http://dx.doi.org/10.1063/1.4979017>]

I. INTRODUCTION

Responsible for electronic dephasing and energy relaxation, the interplay between electronic and nuclear degrees of freedom (DOFs) is a fundamental aspect of dynamical processes in condensed phases such as molecular aggregates and light-harvesting complexes.^{1,2} An accurate description of quantum dissipative dynamics in the condensed phases remains a challenging problem. One of the main schemes for treating quantum dissipation is the reduced density matrix approach, with a focus on truncated system dynamics in the presence of a macroscopic thermal bath. The second-order cumulant time-nonlocal quantum master equation approach^{3–7} and path integral methods such as iterative quasiadiabatic propagator path integral (QUAPI) technique^{8–10} are examples of numerically exact methods for propagating the reduced density matrix. These nonperturbative and non-Markovian approaches allow for exploration of a full range of system-bath coupling and electronic coupling strengths^{5,10} although it becomes extremely difficult to predict quantum dissipative dynamics at very low temperatures.^{11,12} Recent progress in ultrafast time resolved spectroscopy has stimulated methodological developments, and a large number of efficient, approximate reduced density matrix approaches are available.^{13–18}

In the aforementioned reduced density matrix approaches, coupled quantum dynamics of electronic and bosonic degrees of freedom (DOFs) is obtained explicitly only for electronic systems, whereas the bath DOFs are traced out in the

reduced density matrix.² Because of this treatment, all explicit information of the bath dynamics is lost, and the interplay between the system and the bath is only reflected in system observables such as optical spectra and electronic populations. Recent ultrafast nonlinear spectroscopic techniques, such as femtosecond stimulated Raman spectroscopy¹⁹ and two-dimensional electronic-vibrational spectroscopy,²⁰ allow direct monitoring of the temporal evolution of nuclei in the ground or excited electronic states. Hence it becomes increasingly important to address explicit boson dynamics of a many-body boson-electronic system in order to fully interpret nonlinear spectroscopic signals. Alternatively, the wavefunction approaches such as the multiconfigurational time-dependent Hartree (MCTDH) approach^{21,22} and its multilayer variant (ML-MCTDH)^{23–26} can describe time propagation of the wave function of all DOFs explicitly, with equations of motion determined by the Dirac-Frenkel time-dependent variational principle. These approaches are shown to be powerful tools for obtaining numerically exact quantum dynamics at very low temperatures,²⁴ and for including finite temperature effects with the help of statistical sampling of the bath initial conditions.²⁵

One of the established methods for describing time evolution of many-body wave functions is to employ the Dirac-Frenkel time-dependent variational approach with the Davydov *Ansätze*,^{27–29} which consist of sums of direct product states of localized electronic state and coherent states of the bath modes as proposed by Davydov in 1970s to describe soliton motion in molecular chains.³⁰ The time-dependent variational approach with these *Ansätze* has been widely used for describing excitation dynamics and nonlinear optical spectra of Holstein polaron and molecular

^{a)}Electronic address: YZhao@ntu.edu.sg

aggregates.^{31–33} Recently it has been shown that superpositions of the Davydov *Ansätze*, also known as the multiple Davydov *Ansätze*, provide significant improvements in the accuracy of the time-dependent variation.^{34–41} Increasing the multiplicity index in these *Ansätze* leads to numerically exact dynamics in the Holstein model and the sub-Ohmic spin boson model.^{36–38,40} However, the usual variational approach with the Davydov *Ansätze* has been restricted to the zero-temperature restriction because of the wave function formalism.

In this study, we remove the zero-temperature restriction of the variational approach with the Davydov *Ansätze*. For this purpose, we adopt a Monte Carlo like method, inspired by the ML-MCTDH approach.²⁵ The reliability of the extended variational approach with the Davydov *Ansatz* at finite temperature is identified through a comparison with the benchmark results obtained from the QUAPI approach. The rest of the paper is organized as follows. In Sec. II, we introduce the spin-boson Hamiltonian, the Davydov *Ansätze*, and the Monte Carlo importance sampling method. In Sec. III, we present a comparison of population dynamics between ours and the numerically accurate QUAPI results at finite temperatures. Finally, Sec. IV is devoted to concluding remarks.

II. MODEL

A. Hamiltonian

In this study, we consider a two-level system coupled to a single dissipative bath composed of harmonic oscillators as described by the spin-boson model.⁴² The spin-boson model is a paradigm for studying a variety of physical and chemical phenomena such as electron transfer and exciton dynamics in condensed phase systems.^{1,43} Thus, it is a suitable benchmarking system for investigating the validity of the newly developed quantum dynamical approach. The Hamiltonian of the spin-boson model is written as (we set $\hbar = 1$)

$$\hat{H} = \hat{H}_S + \hat{H}_{SB} + \hat{H}_B, \quad (2.1)$$

where

$$\hat{H}_S = \frac{\epsilon}{2}\sigma_z - \frac{\Delta}{2}\sigma_x, \quad (2.2)$$

$$\hat{H}_{SB} = \frac{\sigma_z}{2} \sum_l \lambda_l (b_l^\dagger + b_l), \quad (2.3)$$

$$\hat{H}_B = \sum_l \omega_l b_l^\dagger b_l. \quad (2.4)$$

Here, σ_i ($i = x, z$) are the Pauli operators defined as $\sigma_x = |1\rangle\langle 2| + |2\rangle\langle 1|$ and $\sigma_z = |1\rangle\langle 1| - |2\rangle\langle 2|$ with $|1\rangle$ and $|2\rangle$ representing two localized electronic states. ϵ and Δ are the energy bias and the coupling constant between two electronic states, respectively. b_l^\dagger (b_l) is the creation (annihilation) operator for the bosonic bath mode of frequency ω_l , and λ_l is the strength of the coupling between the system and the l th mode.

Owing to Wick's theorem,^{44,45} the bath-induced process can be specified fully by a two-body correlation function based on $\hat{u}(t) \equiv e^{i\hat{H}_B t} \sum_l \lambda_l (b_l^\dagger + b_l) e^{-i\hat{H}_B t}$ as follows:⁴⁶

$$\begin{aligned} C(t) &= \langle \hat{u}(t) \hat{u}(0) \rangle_B \\ &= \int_0^\infty d\omega J(\omega) [\coth(\beta\omega/2) \cos \omega t - i \sin \omega t], \end{aligned} \quad (2.5)$$

where $\langle \dots \rangle_B$ denotes averaging over $\hat{\rho}_B^{\text{eq}} = e^{-\beta \hat{H}_B} / \text{Tr}_B \{ e^{-\beta \hat{H}_B} \}$ with $\beta = k_B T$ being the inverse temperature. The bath spectral density is defined in terms of the coupling strength λ_l as²

$$J(\omega) = \sum_l \lambda_l^2 \delta(\omega - \omega_l). \quad (2.6)$$

Several forms of $J(\omega)$ are employed in the literature based on model assumptions. In this study, we adopt the following spectral density form:

$$J(\omega) = 2\alpha\omega_c^{1-s}\omega^s e^{-\omega/\omega_c}, \quad (2.7)$$

where α represents the strength of the coupling and ω_c provides a phenomenological frequency cutoff. Those spectral densities with $s < 1$, $s = 1$, and $s > 1$ are referred to as sub-Ohmic, Ohmic, and super-Ohmic, respectively.⁴²

To obtain numerical solutions to the equations of motion for the variational parameters, the continuum spectral density needs to be discretized. The conventional logarithmic discretization method has been employed to investigate the sub-Ohmic spin-boson model at zero temperature,^{34–36,47} but may not be appropriate for finite temperatures. The logarithmic discretization method samples more in the low frequency domain and can better characterize the low frequency bath modes at zero temperature than other discretization schemes. On the other hand, the high frequency bath modes should also be of importance at finite temperatures due to their initial excitations according to the Bose statistics. For this reason, we adopt the spectral density discretization procedure in the ML-MCTDH approach.^{23,24} Following Ref. 24, we introduce a density of frequencies $\Xi(\omega)$ defined on $[0, \omega_{\text{max}}]$, where ω_{max} is the upper bound of the frequency, and discretize the continuum of frequencies as

$$\int_0^{\omega_l} d\omega \Xi(\omega) = l, \quad l = 1, 2, \dots, N_b, \quad (2.8)$$

where N_b is the number of discrete bath modes and $\omega_{N_b} = \omega_{\text{max}}$. The parameter λ_l for each ω_l is then given by $\lambda_l = \sqrt{J(\omega_l)/\Xi(\omega_l)}$. The precise functional form of $\Xi(\omega)$ does not affect the final outcome if sufficient bath modes are included. For efficient numerical calculations, however, the form of $\Xi(\omega)$ can be chosen as

$$\Xi(\omega) = \frac{1}{\Gamma_{\omega_{\text{max}}}} \frac{J(\omega)}{\omega}, \quad (2.9)$$

where

$$\Gamma_{\omega_{\text{max}}} = \frac{1}{N_b} \int_0^{\omega_{\text{max}}} d\omega \frac{J(\omega)}{\omega}. \quad (2.10)$$

Here, $\Gamma_{\omega_{\text{max}}}$ is the factor guaranteeing $\int_0^{\omega_{\text{max}}} d\omega \Xi(\omega) = N_b$. For the Ohmic bath ($s = 1$), ω_l is expressed as $\omega_l = -\omega_c \ln(1 - l\Gamma_{\omega_{\text{max}}}/\omega_c)$. For the sub-Ohmic bath ($s < 1$), ω_l can only be given implicitly through Eq. (2.8).

It is noted that an arbitrary spectral density can be employed in our variational approach. However, handling the spectral density with a complex structure may require a large number of discretized bath modes or a sophisticated discretization procedure. Thus, for simplicity we restrict our numerical

calculations to the functional form of Eq. (2.7), since the goal of our study is to demonstrate the validity of our finite temperature approach.

B. Time dependent variational approach with multiple Davydov trial states

In general, the time evolution of the wave function $|\psi(t)\rangle$ for the total Hamiltonian, \hat{H} , is described with the Schrödinger equation

$$i \frac{\partial}{\partial t} |\psi(t)\rangle = \hat{H} |\psi(t)\rangle. \quad (2.11)$$

In this work, we employ two trial wave functions, namely, the multiple D₁ and D₂ *Ansatz*, to solve the above Schrödinger equation. Both are known as the multiple Davydov *Ansätze* in the hierarchy of the Davydov states. An extension to the single D₁ *Ansatz*, the multiple D₁ *Ansatz* has been employed to investigate both static and dynamical properties of many-body quantum systems such as the spin-boson model and the Holstein molecular crystal model.^{35–37} The time-dependent version of the multi-D₁ *Ansatz* can be written as

$$\begin{aligned} |D_1^M(t)\rangle = & |1\rangle \sum_{n=1}^M A_n(t) \exp\left(\sum_l f_{nl}(t) b_l^\dagger - \text{H.c.}\right) |0\rangle_B \\ & + |2\rangle \sum_{n=1}^M B_n(t) \exp\left(\sum_l g_{nl}(t) b_l^\dagger - \text{H.c.}\right) |0\rangle_B, \end{aligned} \quad (2.12)$$

where $|0\rangle_B$ is the vacuum state of the boson bath. The variational parameters $A_n(t)$ and $B_n(t)$ are the amplitudes in states $|1\rangle$ and $|2\rangle$, respectively. $f_{nl}(t)$ and $g_{nl}(t)$ represent bath-mode displacements with n and l denoting the n th coherent state and the l th bath mode, respectively. M is the multiplicity which denotes the number of single D₁ states in Eq. (2.12). For $M = 1$, the multi-D₁ *Ansatz* reduces to the standard Davydov D₁ *Ansatz*. Similarly, the multi-D₂ *Ansatz* is given by^{39,40}

$$\begin{aligned} |D_2^M(t)\rangle = & |1\rangle \sum_{n=1}^M A_n(t) \exp\left(\sum_l f_{nl}(t) b_l^\dagger - \text{H.c.}\right) |0\rangle_B \\ & + |2\rangle \sum_{n=1}^M B_n(t) \exp\left(\sum_l f_{nl}(t) b_l^\dagger - \text{H.c.}\right) |0\rangle_B \end{aligned} \quad (2.13)$$

where $f_{nl}(t)$ are the displacements of the l th bath mode on any electronic states. Thus, the multi-D₂ *Ansatz* is a simplified version of the multi-D₁ *Ansatz*, since the bath displacements of the multiple D₁ (D₂) trial state is site-dependent (site-independent). For $M = 1$, the multi-D₂ *Ansatz* reduces to the single D₂ *Ansatz*.

The time-dependent variational parameters, $A_n(t)$, $B_n(t)$, $f_{nl}(t)$, and $g_{nl}(t)$, are determined by adopting the Lagrangian formalism of the Dirac-Frenkel time-dependent variational principle. The Lagrangian associated with the trial state $|D_1^M(t)\rangle$ is given by

$$L = \frac{i}{2} \langle D_1^M(t) | \frac{\partial}{\partial t} | D_1^M(t) \rangle - \langle D_1^M(t) | \hat{H} | D_1^M(t) \rangle, \quad (2.14)$$

where the operator $\overleftrightarrow{\partial/\partial t}$ denotes $\overrightarrow{\partial/\partial t} - \overleftarrow{\partial/\partial t}$. The Dirac-Frenkel time-dependent variational principle yields the equations of motion for the variational parameters,

$$\frac{d}{dt} \left(\frac{\partial L}{\partial \dot{u}_n^*} \right) - \frac{\partial L}{\partial u_n^*} = 0, \quad (2.15)$$

where u_n are the variational parameters, i.e., $A_n(t)$, $B_n(t)$, $f_{nl}(t)$, and $g_{nl}(t)$, and u_n^* is the complex conjugate of u_n . Similarly, time evolution for the multi-D₂ *Ansatz* can be derived using the Dirac-Frenkel time-dependent variational principle. Detailed derivations of the equations of motion for the variational parameters of the multiple Davydov *Ansätze* can be found in Ref. 36.

The expectation value of an observable can be expressed as $\langle \hat{O}(t) \rangle = \text{Tr}\{\hat{O} \hat{\rho}_{\text{tot}}(t)\}$, where $\hat{\rho}_{\text{tot}}(t) = e^{-i\hat{H}t} \hat{\rho}_{\text{tot}}(0) e^{i\hat{H}t}$ is the total density operator and \hat{O} is a time independent operator. Using the multi-D₁ or multi-D₂ *Ansatz*, the expectation value of the observable of interest at zero temperature can be calculated as

$$\langle \hat{O}(t) \rangle = \langle D_{1,2}^M(t) | \hat{O} | D_{1,2}^M(t) \rangle. \quad (2.16)$$

In Subsection II C, this expression is extended to the finite temperatures.

C. Observables at finite temperature

The conventional time-dependent variation described above is only applicable at zero temperature. In this subsection, we extend this variational approach to finite temperatures by adopting a Monte Carlo like method, similar to what is used in the ML-MCTDH approach.^{24,25} The initial density matrix for the entire system is assumed to have a factorized form, i.e., $\hat{\rho}_{\text{tot}}(0) = \hat{\rho}(0) \hat{\rho}_B^{\text{eq}}$, where $\hat{\rho}(0) = |1\rangle\langle 1|$. The extension to more general initial conditions with superposition of $|2\rangle$ and $|1\rangle$ is straightforward, which is important for modeling nonlinear spectroscopy.

The expectation value of an observable $\hat{O}(t)$ at finite temperatures can be expressed as

$$\langle \hat{O}(t) \rangle = \text{Tr}\{\hat{O} e^{-i\hat{H}t} \hat{\rho}_B^{\text{eq}} |1\rangle\langle 1| e^{i\hat{H}t}\}. \quad (2.17)$$

In principle, the observables at t can be calculated in any representations. We employ the coherent state representation to calculate the observable as

$$\langle \hat{O}(t) \rangle = \pi^{-N_b} \int d^2\alpha \langle \alpha | \langle 1 | \hat{\rho}_B^{\text{eq}} e^{i\hat{H}t} \hat{O} e^{-i\hat{H}t} | 1 \rangle | \alpha \rangle, \quad (2.18)$$

where $|\alpha\rangle$ denotes a direct product of coherent states $(\alpha_1, \alpha_2, \alpha_3, \dots, \alpha_{N_b})$ for the N_b discrete bath modes and is expressed as $|\alpha\rangle = \exp(\sum_l \alpha_l b_l^\dagger - \text{H.c.}) |0\rangle_B$. Each α_i runs over all feasible coherent states. The element of area $d^2\alpha_i$ on the complex plane of α_i denotes $d\text{Re}(\alpha_i) d\text{Im}(\alpha_i)$, where $\text{Re}(\alpha_i)$ and $\text{Im}(\alpha_i)$ are the real and imaginary parts of α_i , respectively. The equilibrium density matrix of the bath at a finite temperature is a diagonal matrix and can be expressed as^{48,49}

$$\hat{\rho}_B^{\text{eq}} = \int d^2\alpha p(\alpha; \beta) |\alpha\rangle\langle \alpha|, \quad (2.19)$$

where $p(\alpha; \beta)$ represents the diagonal elements of the density matrix in the coherent state representation and can be expressed as⁵⁰

$$p(\alpha; \beta) = \prod_l^{N_b} \left[\frac{e^{\beta\omega_l} - 1}{\pi} \exp(-|\alpha_l|^2(e^{\beta\omega_l} - 1)) \right]. \quad (2.20)$$

As shown in Eq. (2.20), $p(\alpha; \beta)$ is a positive-definite function of α and can be seen as a probability density. Substituting Eq. (2.19) into Eq. (2.18), the observables $\langle O(t) \rangle$ at a finite temperature can be obtained by the average according to the probability density $p(\alpha; \beta)$ as

$$\begin{aligned} \langle \hat{O}(t) \rangle &= \int d^2\alpha p(\alpha; \beta) \langle \alpha | \langle 1 | e^{i\hat{H}t} \hat{O} e^{-i\hat{H}t} | 1 \rangle | \alpha \rangle \\ &= \int d^2\alpha p(\alpha; \beta) \langle D_{1,2}^M(t; \alpha) | \hat{O} | D_{1,2}^M(t; \alpha) \rangle. \end{aligned} \quad (2.21)$$

For the second equality, we have used the multi-D₁ or D₂ Ansatz, $|D_{1,2}^M(t; \alpha)\rangle = e^{-i\hat{H}t} |1\rangle |\alpha\rangle$, and $|D_{1,2}^M(0; \alpha)\rangle$ denotes a trial state with initial bath displacements of α at $t=0$. For the case of the multi-D₁ Ansatz, initial condition parameters are $A_1(0)=1$, $B_1(0)=0$, $A_n(0)=B_n(0)=0$ for $n \neq 1$ and $f_{nl}(0)=g_{nl}(0)=\alpha_l$ for all n and l . Likewise, initial parameters of the multi-D₂ Ansatz are $A_1(0)=1$, $B_1(0)=0$, $A_n(0)=B_n(0)=0$ for $n \neq 1$ and $f_{nl}(0)=\alpha_l$ for all n and l .

The expectation value of the observable at a finite temperature can be obtained numerically by the technique of Monte Carlo importance sampling as

$$\langle \hat{O}(t) \rangle = \frac{1}{N_s} \sum_i^{N_s} \langle D_{1,2}^M(t; \alpha_i) | \hat{O} | D_{1,2}^M(t; \alpha_i) \rangle, \quad (2.22)$$

where N_s is the sampling number. The configuration α_i for the bath is numerically generated according to $p(\alpha; \beta)$ by importance sampling, where $p(\alpha; \beta)$ is the Boltzmann distribution used as the weighting function in the importance sampling procedure. Letting $2\sigma_l^2 = 1/(e^{\beta\omega_l} - 1)$ and $\alpha_l = x_l + ip_l$, $p(\alpha; \beta)$ in Eq. (2.20) can be partitioned into two independent Gaussian distributions as

$$p(\alpha; \beta) = \prod_l^{N_b} \frac{1}{\sqrt{2\pi}\sigma_l} e^{-\frac{x_l^2}{2\sigma_l^2}} \frac{1}{\sqrt{2\pi}\sigma_l} e^{-\frac{p_l^2}{2\sigma_l^2}}, \quad (2.23)$$

where σ_l can be taken as the variance of the Gaussian distribution. To avoid singularity, the initial displacements in the trial states is determined by setting $f_{nl}(0)=g_{nl}(0)=\alpha_l + \epsilon_0$, where noise ϵ_0 satisfying the uniform distribution $[-10^{-2}, 10^{-2}]$ is added to the variational parameters of the initial states. From the definition of σ_l , a lower temperature or a higher frequency ω_l gives a smaller σ_l . The zero temperature case corresponds to every bath mode being in the ground state initially, and it is equivalent to a coherent state with displacement parameter, $\alpha_l=0$ for all l . In this case, the observable expression of Eq. (2.21) or (2.22) reduces to Eq. (2.16).

III. RESULTS AND DISCUSSION

In this section, we compare results from our variational approach with those from the QUAPI method⁸⁻¹⁰ in order to demonstrate the applicability of our approach to unraveling many-body dynamics. In the spin-boson model, a principal

observable of interest is the population difference between the electronic states, $P_z(t)$, calculated as

$$P_z(t) = \langle \sigma_z(t) \rangle = \frac{1}{N_s} \sum_i^{N_s} \langle D_{1,2}^M(t; \alpha_i) | \sigma_z | D_{1,2}^M(t; \alpha_i) \rangle. \quad (3.1)$$

All units in the numerical calculations are scaled by the cut-off frequency ω_c . In this section, for simplicity, we choose zero bias as a large energy bias requires a large multiplicity.⁵¹ The electronic coupling constant and the coupling strength of the spectral density are set as $\Delta=0.1\omega_c$ and $\alpha=0.05$, respectively. The number of the discrete bath modes is fixed at $N_b=250$. In all numerical calculations of this study, statistical averages are taken over a maximum of 400 realizations, which is the number sufficient for convergence at $k_B T = 0.2\omega_c$. For lower temperatures, the observables converge with less realizations.

Here, we briefly mention the numerical convergence of the QUAPI procedure. The basic idea here is to consider a Trotter splitting of the short-time propagator for the total Hamiltonian into one part depending on the system Hamiltonian and another involving the bath and the system-bath coupling term.⁸⁻¹⁰ The short-time density matrix propagator describes time evolution over a time slice Δt . This splitting is exact by construction in the limit of $\Delta t \rightarrow 0$. With the finite time slice Δt in practical calculations, numerical error can be eliminated by choosing sufficiently small Δt to achieve convergence. On the other hand, the bath DOFs generate bath correlations in the Feynman-Vernon influence functional. For any finite temperature, these correlations decay with a dephasing time constant of ω_c^{-1} , thus a memory time window, $\tau_{\text{mem}} = k_{\text{max}}\Delta t$, should be defined to handle the bath correlation truncation beyond a certain time span. Neglected beyond τ_{mem} , all correlations are included exactly within a finite memory time of τ_{mem} . To reach convergence, the memory time window should be enlarged by increasing k_{max} such that all memory effects are taken into account up to a desired accuracy. The QUAPI procedure fails to converge when the memory time is too long. The accuracy of the truncation of k_{max} in Figs. 1 and 2 was checked to make sure that numerical results are converged. In this work, the time slice and the size of the memory window are set to be $\Delta t = 0.125$ and $k_{\text{max}} = 7$, respectively. The convergence failure of the QUAPI method in the deep sub-Ohmic regime is discussed in Section III B.

A. The Ohmic regime

Figures 1(a) and 1(b) display time evolution of $P_z(t)$ calculated by the multi-D₁ Ansatz, the multi-D₂ Ansatz, and the QUAPI approach in the Ohmic case ($s=1$) at two temperatures ($k_B T/\omega_c = 0.01$ and $k_B T/\omega_c = 0.2$), respectively. There is perfect agreement between the D₂^{M=3} Ansatz and the QUAPI approach at the low temperature of $k_B T/\omega_c = 0.01$, as shown in the right panel of Fig. 1(a). On the other hand, the agreement between the D₂^{M=1} Ansatz and the QUAPI approach is unsatisfactory. As discussed in Ref. 36, this is because time evolution of the phonon wave functions shows the plane wave-like behavior in the weak coupling regime and is difficult to be described by superposition of coherent states. Thus, more

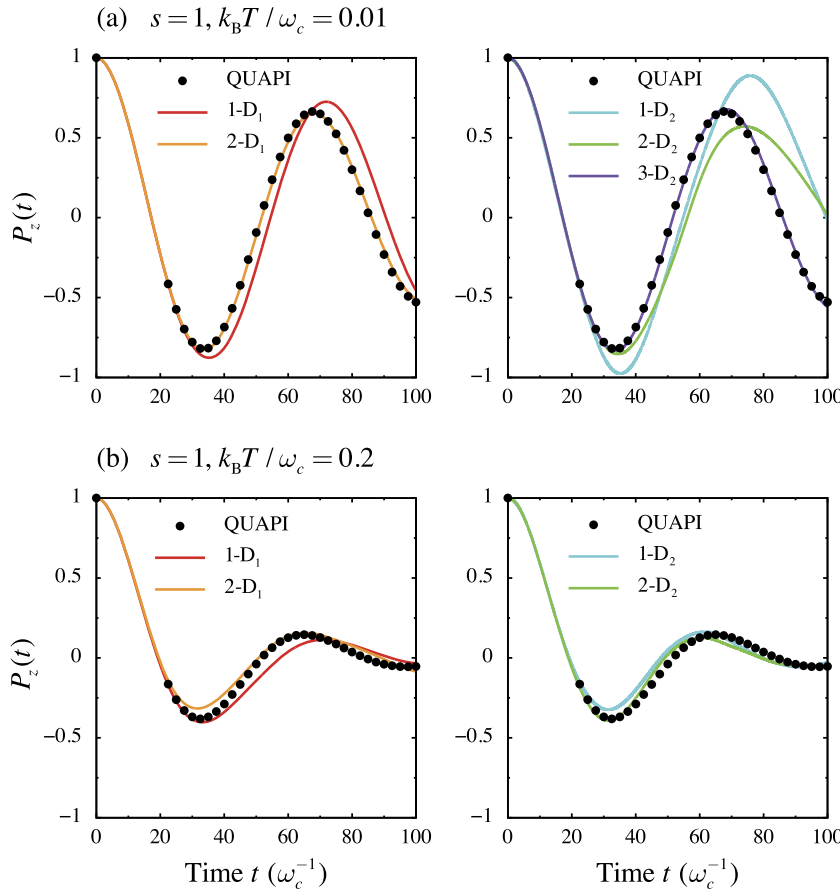


FIG. 1. Time evolution of the population difference $P_z(t)$ in the Ohmic regime ($s = 1$). The factorized bath initial condition is employed. The results calculated by the multi- D_1 *Ansätze* (left panels, solid lines in red and orange) and the multi- D_2 *Ansätze* (right panels, solid lines in blue, green, and purple) are plotted for (a) low temperature ($k_B T / \omega_c = 0.01$) and (b) high temperature cases ($k_B T / \omega_c = 0.2$). The black circles indicate the QUAPI results with $\Delta t = 0.125$ and $k_{\max} = 7$. The other parameters are fixed to be $\epsilon = 0$, $\Delta = 0.1\omega_c$, and $\alpha = 0.05$.

phonon coherent states are needed to capture the accurate dynamics. The multi- D_1 *Ansatz* provides accurate population dynamics by $M=2$, and the agreement between the multi- D_1 *Ansatz* and the QUAPI approach is good even at $M=1$. This clearly demonstrates that the multi- D_1 *Ansätze* are more flexible than the multi- D_2 *Ansätze*.

In the left panel of Fig. 1(b), dynamics obtained by both the $D_1^{M=2}$ *Ansatz* and the QUAPI approach agree with each other at the high temperature ($k_B T / \omega_c = 0.2$) despite a small difference between the $D_1^{M=2}$ *Ansatz* and QUAPI populations. The result by the $D_1^{M=1}$ *Ansatz* also appears to be similar to that by the $M=2$ case. The small difference between the multi- D_1 *Ansätze* and the QUAPI approach may be due to insufficient number of bath modes. From Eq. (2.23) and the definition of the variance of the Gaussian distribution σ_l , the value of σ_l becomes large at high temperatures. The increase of σ_l leads to large values of $f_{nl}(0)$ and $g_{nl}(0)$ even for high frequency modes which can be ignored at low temperatures. Therefore, the number N_b of bath modes required as well as the sampling number becomes large due to a large value of σ_l at high temperatures. The accuracy of the D_2 *Ansatz* with $M=1$ at high temperature is improved significantly unlike in the low temperature regime and is similar to that of the $D_1^{M=2}$ *Ansatz*. These results indicate that the superposition of the Davydov trial states is more fragile against thermal fluctuations at higher temperatures, and thus the trial states with a small multiplicity are sufficient for description of dynamics in this regime. The increased computational cost due to additional bath modes and extended sampling is offset by the reduced *Ansatz* multiplicity,

and thus our variational approach with importance sampling remains efficient even at high temperatures.

B. The sub-Ohmic regime

In this subsection, we focus on the sub-Ohmic regime. Figures 2(a) and 2(b) present the results of $s = 0.8$ at $k_B T / \omega_c = 0.01$ and $k_B T / \omega_c = 0.2$, respectively. These results demonstrate that the variational approach with the multi- D_1 *Ansätze* provides excellent dynamics simulation over a range of temperatures and bath spectral exponents s . Calculated dynamics in Fig. 2 shows the fast coherence decay compared to the Ohmic bath case, although the sub-Ohmic regime corresponds to slow bath relaxation. This fast coherence decay can be explained as follows. A direct measure of the coupling strength between the system and the bath is the bath reorganization energy, $E_r = \int_0^\infty d\omega J(\omega)/\omega$, which represents the dissipated environment energy after electronic excitation in accordance with the vertical Franck-Condon transition in the electron transfer theory.¹⁴ From the definition of the spectral density of Eq. (2.7), the value of E_r in the case of $s = 0.8$ is large compared with the Ohmic bath case when other parameters except the value of s are fixed. A large E_r corresponds to large fluctuations according to the fluctuation-dissipation relation,^{14,46} which eradicate electronic coherence similar to what occurs in the Ohmic case. This physical explanation is consistent with the numerical fact that the required multiplicity in both multi- D_1 and multi- D_2 *Ansätze* in the case of $s = 0.8$ is not dissimilar to the Ohmic case.

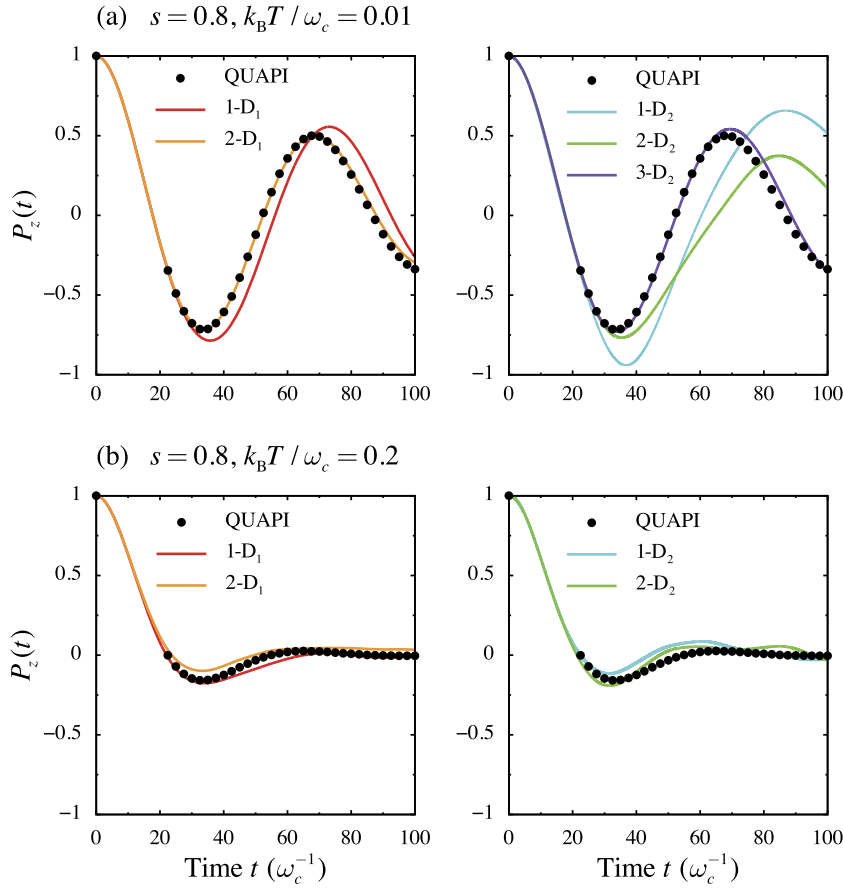


FIG. 2. Time evolution of the population difference $P_z(t)$ with spectral density exponent $s=0.8$. The factorized bath initial condition is employed. The results calculated by the multi- D_1 *Ansätze* (left panels, solid lines in red and orange) and the multi- D_2 *Ansätze* (right panels, solid lines in blue, green, and purple) are plotted for two cases (a) low temperature ($k_B T / \omega_c = 0.01$) and (b) high temperature ($k_B T / \omega_c = 0.2$). The black circles indicate the QUAPI results with $\Delta t = 0.125$ and $k_{\max} = 7$. The other parameters are fixed to be $\epsilon = 0$, $\Delta = 0.1\omega_c$, and $\alpha = 0.05$.

Finally, we discuss potential applicability of the multiple Davydov *Ansätze* in the deep sub-Ohmic regime ($s < 0.5$), which corresponds to situations with the ultra slow bath relaxation. In the slow bath regime, it is known that some notable discrepancies exist between exact results and those from the QUAPI procedure at long times, as discussed in Ref. 12. To obtain correct long time dynamics, one would need to increase the memory window size k_{\max} , making QUAPI convergence more difficult to achieve. It has been demonstrated that the multi- D_1 *Ansatz* is consistent with the results from the second-order cumulant time-nonlocal quantum master equation and the real-time path integral Monte Carlo approaches for $s = 0.25$ at zero temperature and is a reliable, efficient method for describing quantitatively accurate dynamics of the deep

sub-Ohmic regime.³⁶ From Figs. 1 and 2, the validity of the multiple Davydov *Ansätze* at finite temperatures also seems to be independent of the exponent s , but the required multiplicity may depend on it. In order to clarify the relation between the spectral exponent and the required multiplicity, we explore a case with an exponent s smaller than that in Fig. 2. As a helpful reference, we also compare our results with those from the thermal field dynamics (TFD),⁵² similar to the approach of Borrelli and Gelin.⁵³ Figure 3 presents results of $s = 0.6$ at $k_B T / \omega_c = 0.01$. The dynamics from the $D_1^{M=2}$ *Ansatz* is in perfect agreement with those of QUAPI and TFD, as shown in left panel of Fig. 3. As demonstrated in the right panel of Fig. 3, it is found that the multi- D_2 *Ansatz* slightly overestimates the amplitude of population oscillation at $M = 3$, and one

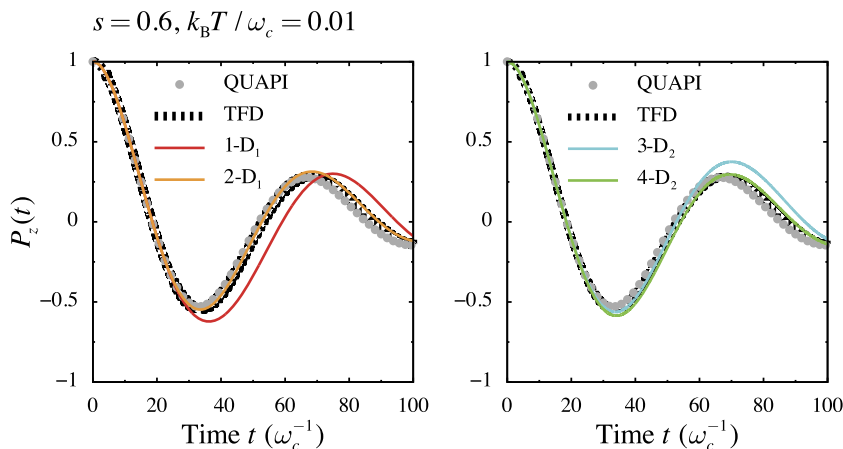


FIG. 3. Time evolution of the population difference $P_z(t)$ with spectral density exponent $s=0.6$. The factorized bath initial condition is employed. The results calculated by the multi- D_1 *Ansätze* (left panels, solid lines in red and orange) and the multi- D_2 *Ansätze* (right panels, solid lines in blue and green) are plotted for low temperature case ($k_B T / \omega_c = 0.01$). The gray circles indicate the QUAPI results with $\Delta t = 0.125$ and $k_{\max} = 8$. The TFD approach with $D_1^{M=4}$ *Ansatz* (dashed line in black) is plotted. The other parameters are fixed to be $\epsilon = 0$, $\Delta = 0.1\omega_c$, and $\alpha = 0.05$.

needs to increase the multiplicity further to $M = 4$ for numerical convergence. Fortunately, no large increase in the multiplicity of the multi- D_2 *Ansatz* is needed for adequate convergence with decreasing s . To explore how the required multiplicity is affected by thermal fluctuations, we have considered a case of relatively small system-bath coupling strength α in all numerical calculations of this study. From some previous studies of the multiple Davydov *Ansätze*,^{36,37} it has been found that the required multiplicity is reduced by increasing the system-bath coupling strength because the large bath-induced fluctuations eradicate the need for deep superposition of single Davydov states. Especially in the moderate to strong coupling regimes, our results suggest that both the multi- D_1 and the multi- D_2 *Ansätze* hold an advantage over the QUAPI method in the sub-Ohmic regime, where our approach is not burdened with significantly increased computational cost as the spectral density exponent s is reduced. Therefore, the multiple Davydov *Ansätze* including temperature effects is expected to be a reliable, efficient tool for exploring quantum dynamics in the sub-Ohmic regime at both low and high temperatures.

IV. CONCLUDING REMARKS

In this study, we have extended the Dirac-Frenkel time-dependent variational approach with the Davydov *Ansätze* to finite temperatures by adopting the Monte Carlo importance sampling method. To demonstrate the applicability of this approach, we have compared real-time quantum dynamics of the spin-boson model calculated by our approach with that from the numerically exact QUAPI approach. It is shown that our variational approach with the multiple Davydov *Ansätze* is accurate over a range of temperatures and bath spectral densities. Variational dynamics with the single Davydov *Ansatz* shows excellent agreement with the QUAPI results at high temperatures, while the difference between both approaches becomes significant at low temperatures. Accuracy in dynamical calculations employing multiple Davydov trial states is improved significantly over the single Davydov *Ansatz*, especially in the low temperature regime. The reduction in the *Ansatz* multiplicity due to thermal fluctuations cancels out the computational cost increase due to an increased number of bath modes and extended sampling at high temperatures, and thus our variational technique with importance sampling remains efficient even at an elevated temperature. Our results in the sub-Ohmic regime demonstrate a great advantage of the variational approach with the multiple Davydov *Ansätze* because conventional perturbative approaches fail to describe strongly non-Markovian dynamics due to the long-time tail of the time correlation function of the sub-Ohmic bath. Our variational approach including temperature effects is expected to open up new avenues of probing quantum dynamics in the sub-Ohmic regime.

The novel advantage of the wave function propagation methods is to give access to the dynamics of all bath DOFs explicitly.^{29,39,41,54,55} Kühn and co-workers have investigated impacts of quantum mechanically mixed electronic and vibrational states on electronic energy transfer dynamics in the Fenna-Matthews-Olson pigment-protein complex by tracking time evolution of bath DOFs based on the ML-MCTDH

approach.^{54,55} Their calculations clearly showed the importance of vibrational motion on local electronic ground states in the quantum mixing of electronic and vibronic excitations, which is consistent with the argument in Ref. 6. However, the zero temperature assumption may lead to unreliable predictions for their role at physiological temperatures because the mixed electronic and vibrational states are fragile against thermal fluctuations.⁶ Our finite-temperature time-dependent variational approach with the multiple Davydov states is demonstrated to remain efficient even at an elevated temperature, and thus can explore effects of thermal fluctuations on the mixed electronic-vibrational states by tracking dynamics of vibrational DOFs.

The time-dependent variational approach with importance sampling requires averaging over a large number of realizations at high temperatures, which may increase the computational cost in comparison with zero-temperature cases despite that the multiplicity M required for convergence decreases with the increasing temperature. Developing efficient techniques of importance sampling holds the key to improved statistics. By employing the thermo field dynamics approach,⁵³ the variational approach with the Davydov *Ansätze* can be applied to finite temperature scenarios while avoiding the sampling procedure. A comprehensive study along this direction is currently in progress.⁵²

ACKNOWLEDGMENTS

One of us (L.W.) would like to thank Ke-Wei Sun for helpful discussion. This work was supported by the Singapore National Research Foundation through the Competitive Research Programme (CRP) under Project No. NRF-CRP5-2009-04 and the Singapore Ministry of Education of Education through the Academic Research Fund (Tier 2) under Project No. MOE2014-T2-1-099.

¹A. Nitzan, *Chemical Dynamics in Condensed Phases: Relaxation, Transfer and Reactions in Condensed Molecular Systems* (Oxford University Press, New York, 2006).

²V. May and O. Kühn, *Charge and Energy Transfer Dynamics in Molecular Systems* (Wiley-VCH, Weinheim, 2004).

³Y. Tanimura and R. Kubo, *J. Phys. Soc. Jpn.* **58**, 101 (1989).

⁴A. Ishizaki and Y. Tanimura, *J. Phys. Soc. Jpn.* **74**, 3131 (2005).

⁵A. Ishizaki and G. R. Fleming, *J. Chem. Phys.* **130**, 234111 (2009).

⁶Y. Fujihashi, G. R. Fleming, and A. Ishizaki, *J. Chem. Phys.* **142**, 212403 (2015).

⁷L. Chen, Y. Zhao, and Y. Tanimura, *J. Phys. Chem. Lett.* **6**, 3110 (2015).

⁸N. Makri and D. E. Makarov, *J. Chem. Phys.* **102**, 4600 (1995).

⁹N. Makri and D. E. Makarov, *J. Chem. Phys.* **102**, 4611 (1995).

¹⁰P. Nalbach, A. Ishizaki, G. R. Fleming, and M. Thorwart, *New J. Phys.* **13**, 063040 (2011).

¹¹Z. Tang, X. Ouyang, Z. Gong, H. Wang, and J. Wu, *J. Chem. Phys.* **143**, 224112 (2015).

¹²H. T. Chen, G. Cohen, and D. R. Reichman, e-print [arXiv:1610.09402](https://arxiv.org/abs/1610.09402).

¹³Y.-C. Cheng and G. R. Fleming, *Annu. Rev. Phys. Chem.* **60**, 241 (2009).

¹⁴A. Ishizaki, T. R. Calhoun, G. S. Schlau-Cohen, and G. R. Fleming, *Phys. Chem. Chem. Phys.* **12**, 7319 (2010).

¹⁵S. F. Huelga and M. B. Plenio, *Contemp. Phys.* **54**, 181 (2013).

¹⁶A. Chenu and G. D. Scholes, *Annu. Rev. Phys. Chem.* **66**, 69 (2015).

¹⁷L. Chen, P. Shenai, F. Zheng, A. Somoza, and Y. Zhao, *Molecules* **20**, 15224 (2015).

¹⁸M. K. Lee, P. Huo, and D. F. Coker, *Annu. Rev. Phys. Chem.* **67**, 639 (2016).

¹⁹P. Kukura, D. W. McCamant, and R. A. Mathies, *Annu. Rev. Phys. Chem.* **58**, 461 (2007).

- ²⁰T. A. Oliver, N. H. Lewis, and G. R. Fleming, *Proc. Natl. Acad. Sci. U. S. A.* **111**, 10061 (2014).
- ²¹H.-D. Meyer, U. Manthe, and L. S. Cederbaum, *Chem. Phys. Lett.* **165**, 73 (1990).
- ²²F. Matzkies and U. Manthe, *J. Chem. Phys.* **110**, 88 (1999).
- ²³H. Wang, M. Thoss, and W. H. Miller, *J. Chem. Phys.* **115**, 2979 (2001).
- ²⁴H. Wang and M. Thoss, *J. Chem. Phys.* **119**, 1289 (2003).
- ²⁵H. Wang and M. Thoss, *J. Chem. Phys.* **124**, 034114 (2006).
- ²⁶U. Manthe, *J. Chem. Phys.* **128**, 164116 (2008).
- ²⁷M. J. Škrinjar, D. V. Kapor, and S. D. Stojanović, *Phys. Rev. A* **38**, 6402 (1988).
- ²⁸W. Förner, *Phys. Rev. B* **53**, 6291 (1996).
- ²⁹J. Sun, B. Luo, and Y. Zhao, *Phys. Rev. B* **82**, 014305 (2010).
- ³⁰A. S. Davydov, *Phys. Scr.* **20**, 387 (1979).
- ³¹T. D. Huynh, K. W. Sun, M. F. Gelin, and Y. Zhao, *J. Chem. Phys.* **139**, 104103 (2013).
- ³²V. Chorošajev, A. Gelzinis, L. Valkunas, and D. Abramavicius, *J. Chem. Phys.* **140**, 244108 (2014).
- ³³L. Chen, M. F. Gelin, W. Domcke, and Y. Zhao, *J. Chem. Phys.* **142**, 164106 (2015).
- ³⁴N. Zhou, L. Chen, Y. Zhao, D. Mozyrsky, V. Chernyak, and Y. Zhao, *Phys. Rev. B* **90**, 155135 (2014).
- ³⁵N. Zhou, L. Chen, D. Xu, V. Chernyak, and Y. Zhao, *Phys. Rev. B* **91**, 195129 (2015).
- ³⁶L. Wang, L. Chen, N. Zhou, and Y. Zhao, *J. Chem. Phys.* **144**, 024101 (2016).
- ³⁷N. Zhou, L. Chen, Z. Huang, K. Sun, Y. Tanimura, and Y. Zhao, *J. Phys. Chem. A* **120**, 1562 (2016).
- ³⁸T. Deng, Y. Yan, L. Chen, and Y. Zhao, *J. Chem. Phys.* **144**, 144102 (2016).
- ³⁹N. Zhou, Z. Huang, J. Zhu, V. Chernyak, and Y. Zhao, *J. Chem. Phys.* **143**, 014113 (2015).
- ⁴⁰Z. Huang, L. Wang, C. Wu, L. Chen, F. Grossmann, and Y. Zhao, *Phys. Chem. Chem. Phys.* **19**, 1655 (2017).
- ⁴¹Y. Fujihashi, L. Chen, A. Ishizaki, J. Wang, and Y. Zhao, *J. Chem. Phys.* **146**, 044101 (2017).
- ⁴²A. J. Leggett, S. Chakravarty, A. T. Dorsey, M. P. A. Fisher, A. Garg, and W. Zwerger, *Rev. Mod. Phys.* **59**, 1 (1987).
- ⁴³U. Weiss, *Quantum Dissipative Systems* (World Scientific, Singapore, 1999).
- ⁴⁴G. C. Wick, *Phys. Rev.* **80**, 268 (1950).
- ⁴⁵A. L. Fetter and J. D. Walecka, *Quantum Theory of Many-Particle Systems* (McGraw-Hill, New York, 1971).
- ⁴⁶R. Kubo, M. Toda, and N. Hashitsume, *Statistical Physics II: Nonequilibrium Statistical Mechanics* (Springer, Berlin, Heidelberg, 1985).
- ⁴⁷R. Bulla, N. H. Tong, and M. Vojta, *Phys. Rev. Lett.* **91**, 170601 (2003).
- ⁴⁸R. J. Glauber, *Phys. Rev. Lett.* **131**, 2766 (1963).
- ⁴⁹E. C. G. Sudarshan, *Phys. Rev. Lett.* **10**, 277 (1963).
- ⁵⁰M. Hillery, R. F. O'Connell, M. O. Scully, and E. P. Wigner, *Phys. Rep.* **106**, 121 (1984).
- ⁵¹R. Borrelli and A. Peluso, *J. Chem. Phys.* **144**, 114102 (2016).
- ⁵²L. Chen and Y. Zhao, "Finite-temperature dynamics of a Holstein polaron: Thermofield dynamics approach" (unpublished).
- ⁵³R. Borrelli and M. F. Gelin, *J. Chem. Phys.* **145**, 224101 (2016).
- ⁵⁴J. Schulze and O. Kühn, *J. Phys. Chem. B* **119**, 6211 (2015).
- ⁵⁵J. Schulze, M. F. Shibl, M. J. Al-Marri, and O. Kühn, *J. Chem. Phys.* **144**, 185101 (2016).